Minimum Requirements for Substrates of Mammalian tRNA 3′ Processing Endoribonuclease†

Masayuki Nashimoto,* Masato Tamura,‡ and Roger L. Kaspar

Department of Chemistry and Biochemistry, Brigham Young University, Provo, Utah 84602

Received May 25, 1999; Revised Manuscript Received July 29, 1999

ABSTRACT: Mammalian tRNA 3′ processing endoribonuclease (3′ tRNase) removes a 3′ trailer after the discriminator nucleotide from precursor tRNA (pre-tRNA). To elucidate the minimum requirements for 3′ tRNase substrates, we tested small pre-tRNA^{Arg} substrates lacking the D and anticodon stem−loop domain for cleavage by purified pig 3′ tRNase. A small pre-tRNA (R-ATW) composed of an acceptor stem, an extra loop, a T stem−loop domain, a discriminator nucleotide, and a 3′ trailer was cleaved more efficiently than the full-length wild type. The catalytic efficiencies of three R-ATW derivatives, which were constructed to destroy the original T stem base pairs, were also higher than that of the full-length wild type. Pig 3′ tRNase efficiently processed a "minihelix" (R-ATM5) that consists of a T stem−loop domain, an acceptor stem, a discriminator nucleotide, and a 3′ trailer, while the enzyme never cleaved a "microhelix" that is composed of a T loop, an acceptor stem, a discriminator nucleotide, and a 3′ trailer. Five R-ATM5 derivatives that have one to seven base substitutions in the T loop were all cleaved slightly more efficiently than the full-length wild type and slightly less efficiently than R-ATM5. A helix ("minihelixΔ1") one base pair smaller than minihelices was a good substrate, while small helices containing a continuous 10-base pair stem were poor substrates. The cleavage of these three small substrates occurred after the discriminator and one to three nucleotides downstream of the discriminator. From these results, we conclude that minimum substrates for efficient cleavage by mammalian 3′ tRNase are minihelices or minihelicesΔ1, in which there seem to be no essential bases.

Eukaryotic nuclear tRNAs are transcribed as larger precursors containing 5′ leader and 3′ trailer sequences by RNA polymerase III (*1*). The 5′ end processing of the precursor tRNA (pre-tRNA)[1] is accomplished by RNase P (*2*). Eukaryotic tRNA 3′ processing endoribonuclease (3′ tRNase) is an enzyme responsible for the removal of a 3′ trailer from pre-tRNA (Figure 1) (*3*). RNase P from various eukaryotes and prokaryotes and bacterial exoribonucleases involved in tRNA 3′ processing have been studied extensively (*2, 4*). Much less is known, however, about eukaryotic tRNA 3′ processing.

The endonucleolytic cleavage by eukaryotic 3′ tRNase occurs after the discriminator nucleotide, to which tRNA nucleotidyltransferase adds CCA residues (*5*). The efficiency of tRNA 3′ processing by mammalian 3′ tRNase differs depending on both 3′ trailer length and the 5′ end nucleotide (effector nucleotide) of the 3′ trailer (*3*). Cleavage efficiency decreases in the following order of effector nucleotides: G ∼ A > U > C; the CCA sequence cannot be removed from mature tRNA by mammalian 3′ tRNase (*3, 6*). The distribution of both lengths and effector nucleotides of mammalian pre-tRNA 3′ trailers reflects these 3′ tRNase properties (*3*). The 3′ processing efficiency is also affected by the pre-tRNA 5′ leaders (*7*). We have demonstrated that leaders with nine or more nucleotides strongly inhibit the 3′ processing reaction, and that 5′ leaders even as small as three and six nucleotides, when base-paired with a 3′ trailer, severely hinder removal of the 3′ trailer by 3′ tRNase (*7*).

Recently, we have elucidated a general rule for cleavage site selection by mammalian 3′ tRNase (*8*). Pre-tRNAs with a total of N base pairs ($N < 12$) in the acceptor stem and the T stem are cleaved 13 and 14 nucleotides from the most distal T stem base pair, or $12 - N$ and $13 - N$ nucleotides 3′ to the discriminator (*8*). On the other hand, pre-tRNA variants containing a total of N base pairs ($N \geq 12$) are cleaved only $N + 1$ nucleotides from the most distal T stem base pair (i.e., after the discriminator nucleotide) (*8*).

We have also shown that mammalian 3′ tRNase can recognize and cleave various pre-tRNA-like complexes. These include RNA complexes of ∼65-nucleotide 3′-truncated tRNAs and RNAs containing a sequence complementary to the first four nucleotides of the 3′-truncated tRNAs (*9*−*11*), and RNA complexes of 5′ half-tRNAs (the 5′ end to the anticodon) and 3′ half-tRNAs (the anticodon to the discriminator and the 3′ trailer) (*12*). Furthermore, we have demonstrated that the small RNA complex of T3H and the heptamer T7M7 containing an acceptor stem, a T stem−loop domain, and a 3′ trailer is a good substrate for mammalian 3′ tRNase (*13*). The cleavage efficiency of small RNA complexes decreases as the number of T stem base

† This work was supported by the Bireley Foundation and U.S. Public Health Service Grant GM57644 from the National Institutes of Health.

* To whom correspondence should be addressed. Telephone: (801) 378-8667. Fax: (801) 378-5474. E-mail: mnashimoto@chemgate.byu.edu.

‡ Present address: Department of Biochemistry, Kagoshima University Dental School, Kagoshima 890-8544, Japan.

[1] Abbreviations: pre-tRNA, precursor tRNA; 3′ tRNase, tRNA 3′ processing endoribonuclease.

10.1021/bi9911942 CCC: $18.00
Published on Web 08/20/1999

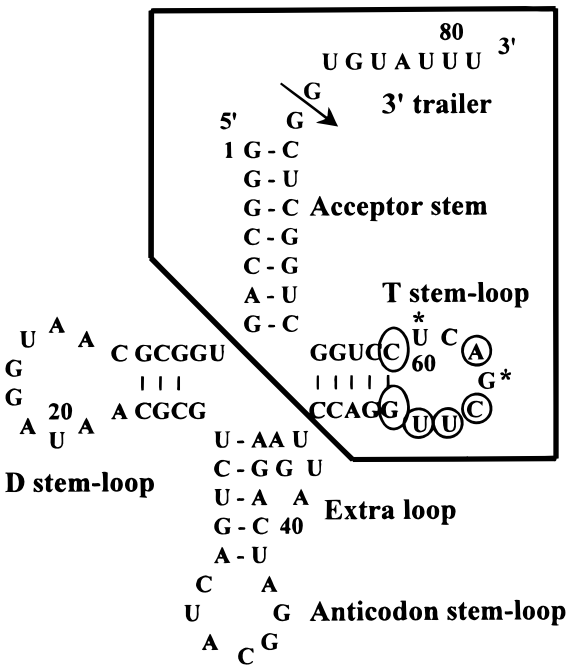

Pre-tRNA^{Arg} R-UUU

FIGURE 1: Secondary structure of the wild-type pre-tRNA^{Arg} R-UUU. The site of cleavage by 3′ tRNase is denoted with an arrow. This study focuses on the boxed structure. Circles and asterisks denote conserved and semiconserved nucleotides, respectively, in the T stem−loop domain.

pairs decreases, and 3′ tRNase cannot cleave the RNA complex of T7HM3 and T7M7 lacking a T stem structure (*13*).

In previous experiments, we could not compare the catalytic efficiency of the small RNA complexes with that of the wild-type pre-tRNA^{Arg} R-UUU (Figure 1) because only the products of the K_m and K_d values for the RNA complexes were obtained (*13*). In this paper, to compare cleavage efficiencies directly, we tested small pre-tRNA^{Arg} substrates of single molecules for 3′ tRNase cleavage, and determined the kinetic parameters K_m and V_{max}. Furthermore, we investigated minimum requirements for substrates of mammalian 3′ tRNase.

MATERIALS AND METHODS

Pre-tRNA Synthesis. We obtained partially double-stranded DNA templates by annealing synthetic DNAs containing a T7 promoter followed by complementary sequences to small pre-tRNA^{Arg}s with a 17-nucleotide T7 promoter oligodeoxynucleotide (5′-TAATACGACTCACTATA-3′) in 10 mM Tris-HCl (pH 7.5) and 10 mM $MgCl_2$. The pre-tRNAs were synthesized with T7 RNA polymerase (Promega and Takara Shuzo) from these templates. The transcription was carried out in the presence or absence of [α-^{32}P]UTP (DuPont NEN) under the conditions recommended by the manufacturer (Promega and Takara Shuzo). The transcribed pre-tRNAs were gel-purified prior to 3′ tRNase assays.

Preparation of Pig 3′ tRNase. We prepared 3′ tRNase from pig liver basically as previously described (*11*). Briefly, homogenates of fresh pig liver were heated at 55 °C for 5 min, and precipitated materials were removed by centrifugation. The supernatant was precipitated with ammonium sulfate (50% saturation). The precipitated samples were subsequently fractionated via Q Sepharose Fast Flow (Pharmacia), Blue Sepharose (Pharmacia), and Heparin Sepharose (Pharmacia) column chromatography. In this paper, instead of a Mono Q column (*11*), we layered the 3′ tRNase fractions after Heparin Sepharose chromatography onto a 10 mL 15 to 30% glycerol gradient in a buffer [20 mM Tris-HCl (pH 7.5) and 0.2 mM EDTA] and centrifuged them at 38 000 rpm for 48 h at 4 °C. The specific activity of the most active fraction used here was almost the same as that of the enzyme after Mono Q column chromatography.

3′ tRNase Assay. The 3′ tRNase reactions for ^{32}P-labeled small pre-tRNAs (0.1 pmol) were performed with the pig 3′ tRNase fraction (3 ng) in a mixture (6 μL) containing 10 mM Tris-HCl (pH 7.5), 1.5 mM dithiothreitol, and 3.2 mM $MgCl_2$ at 37 °C for the indicated periods of time (*3*). After extraction with phenol/chloroform, the reaction products were separated on 10% polyacrylamide−8 M urea gels, and the gels were autoradiographed.

Kinetic Analysis. Cleavage of small pre-tRNA^{Arg}s by 3′ tRNase was examined at various substrate concentrations (*3*). A reaction mixture (6 μL) contained 10 mM Tris-HCl (pH 7.5), 1.5 mM dithiothreitol, 3.2 mM $MgCl_2$, and 0.125−1.7 μM pre-tRNA. The reactions were started by adding pig 3′ tRNase fraction (1 ng) after glycerol gradient centrifugation, and continued at 37 °C for 1 min. The reaction products were resolved on a 10% polyacrylamide−8 M urea gel and then quantitated with a Molecular Imager (Bio-Rad). Values of K_m and V_{max} were obtained from double-reciprocal plots.

3′-End-Labeling and RNA Sequencing. Unlabeled small pre-tRNA transcripts (2 pmol) were reacted with pig 3′ tRNase (6 ng) under the standard assay conditions at 37 °C for 10 min, extracted with phenol/chloroform, and precipitated with ethanol. The reaction products dissolved in water were 3′-end-labeled with [5′-^{32}P]pCp and T4 ligase (Takara Shuzo) at 4 °C for 10 h. The smallest 5′ cleavage products were gel-purified, and their 3′ terminal sequences were determined by the chemical RNA sequencing method with a slight modification of the C+U reaction (*14*).

RESULTS AND DISCUSSION

A Pre-tRNA Variant Lacking the D and Anticodon Stem−Loop Domains Is a Better Substrate than Its Wild Type. First of all, we tested a small pre-tRNA^{Arg} substrate (R-ATW) for 3′ tRNase cleavage (Figure 2A), and determined the kinetic parameters K_m and V_{max}. R-ATW (Figure 2A) was constructed by deleting the D and anticodon stem−loop domain from its wild-type R-UUU (Figure 1). The substrate was synthesized in vitro with T7 RNA polymerase from a synthetic DNA template containing a T7 promoter (*3*). In vitro cleavage assays were performed at 37 °C using purified pig 3′ tRNase as described previously (*3*). As expected, 3′ tRNase cleaved R-ATW efficiently (Figure 2B, lanes 1−4). The kinetic parameters were obtained from cleavage rates at substrate concentrations of 0.125−1.7 μM as described previously (*3*). Interestingly, the K_m for R-ATW was lower than that for R-UUU, and the V_{max} for R-ATW was higher than that for R-UUU (Table 1). As a result, the catalytic efficiency of R-ATW was more than twice as high as that of R-UUU (Table 1). These results confirmed that the D and

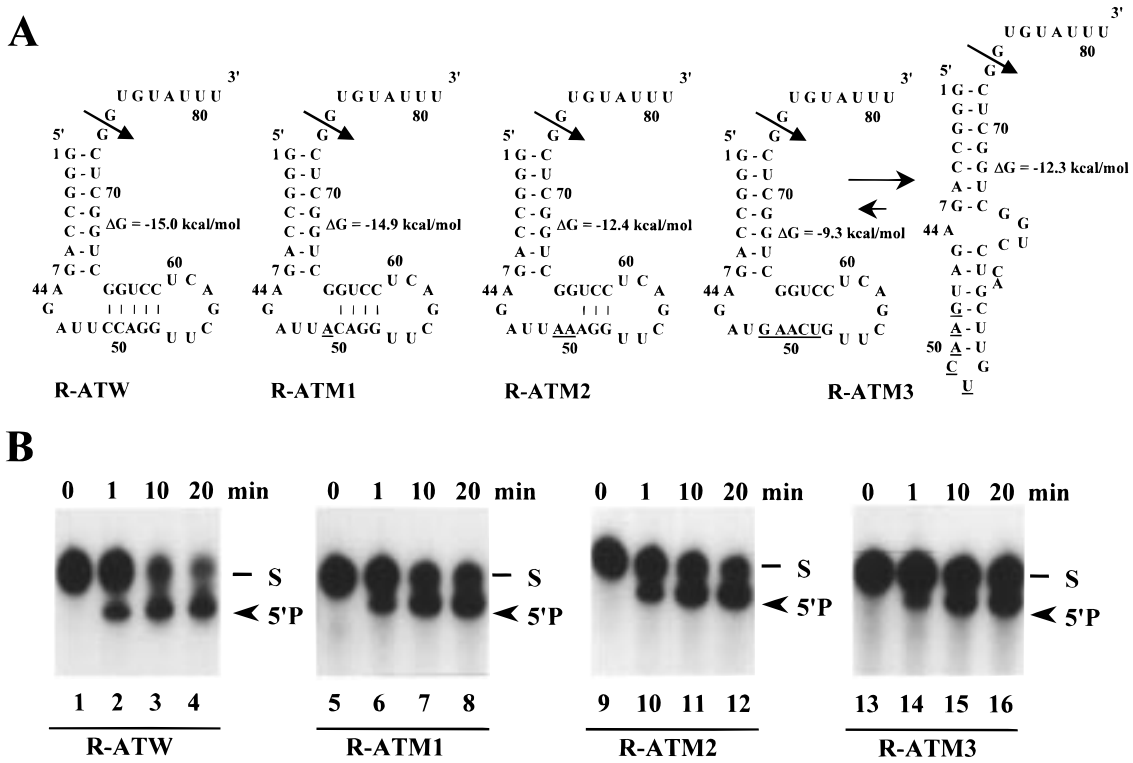

FIGURE 2: Mammalian 3′ tRNase cleavage assays for small pre-tRNA^{Arg} substrates. (A) Secondary structures of small pre-tRNA^{Arg}s, R-ATW, R-ATM1, R-ATM2, and R-ATM3, with their Δ*G* values. The acceptor stem and the T stem−loop domain are connected by the extra loop. In the numbering system used in this paper, nucleotide deletions do not change numbers assigned to each nucleotide of the wild-type pre-tRNA^{Arg} R-UUU (Figure 1). Arrows and underlines denote the sites of cleavage by 3′ tRNase and substituted nucleotides, respectively. (B) 3′ tRNase assays for R-ATW (lanes 1−4), R-ATM1 (lanes 5−8), R-ATM2 (lanes 9−12), and R-ATM3 (lanes 13−16). Each small substrate (0.1 pmol) uniformly labeled with [α-^{32}P]UTP was incubated with a pig 3′ tRNase fraction (3 ng) at 37 °C for the indicated periods of time. The cleavage products were analyzed on 10% polyacrylamide−8 M urea gels. S and 5′P denote small pre-tRNA substrates and 5′ products, respectively. The smaller amount of material seen in lanes 3 and 4 is probably due to the loss of RNA during the RNA recovery procedure.

Table 1: Kinetic Parameters for Cleavage of Small Pre-tRNA^{Arg}s by Pig 3′ tRNase

substrate	K_m[a] (μM)	V_{max}[a] (pmol/min)	relative V_{max}/K_m
R-UUU	0.57	0.65	100
R-ATW	0.41	1.0	214
R-ATM1	0.44	1.4	279
R-ATM2	0.32	1.1	302
R-ATM3	0.59	1.1	163
R-ATM4	0.66	0.82	109
R-ATM5	0.57	0.86	132
R-ATM7	0.58	0.83	125
R-ATM8	0.52	0.71	120
R-ATM9	0.63	0.81	113
R-ATM10	0.65	0.80	108
R-ATM11	0.68	0.93	120

[a] The maximum velocity per nanogram of pig 3′ tRNase fraction after glycerol gradient centrifugation is shown. Each set of kinetic parameters was obtained from a double-reciprocal plot using average velocities of three trials with a standard deviation of 5−13% at different substrate concentrations (0.125−1.7 μM).

anticodon stem−loop domains are not essential for efficient recognition and cleavage by mammalian 3′ tRNase (*13*). *Drosophila* 3′ tRNase has been also shown to cleave a similar small pre-tRNA^{His} as efficiently as the corresponding wild type, although the kinetic parameters for the reactions were not compared (*15*).

Effects of T Stem Base Pair Destruction. We also examined the effect of T stem base pair destruction on cleavage efficiency using three variants of R-ATW. R-ATM1, R-ATM2, and R-ATM3 were constructed to destroy the one, two, and four original T stem base pairs, respectively (Figure 2A). The base substitutions in these variants were located in the same positions as in the T7HM series (*13*). Unexpectedly, 3′ tRNase efficiently removed 3′ trailers from all of those small substrates (Figure 2B). R-ATM1 and R-ATM2 were cleaved more efficiently than R-ATW and ∼3-fold as efficiently as R-UUU (Table 1). Even R-ATM3, which was initially expected to form no base pairs in the T stem domain, had a >1.5-fold higher V_{max}/K_m value than R-UUU (Table 1).

Computer analysis for the RNA secondary structure prediction suggested that R-ATM3 may form a more stable alternative secondary structure with a Δ*G* value of −12.3 kcal/mol (Figure 2A). Additionally, in structure probing for R-ATM3, cleavage by RNase T1 at G53 was very efficient, while sites G45, G48, and G57 were much less susceptible to RNase T1 (data not shown). These observations support the possibility that the alternative structure may be more favorable than the initially expected RNA structure with no base pairs in the T stem domain (Figure 2A).

Although the conclusion that the three variants R-ATM1, R-ATM2, and R-ATM3 are all very good substrates for 3′ tRNase is apparently inconsistent with our previous results obtained for the RNA complexes with T7M7 (*13*), this can be explained by taking into account differences in the whole structure. In the case of the R-ATM series, the acceptor stem and the T stem−loop domain are covalently connected at

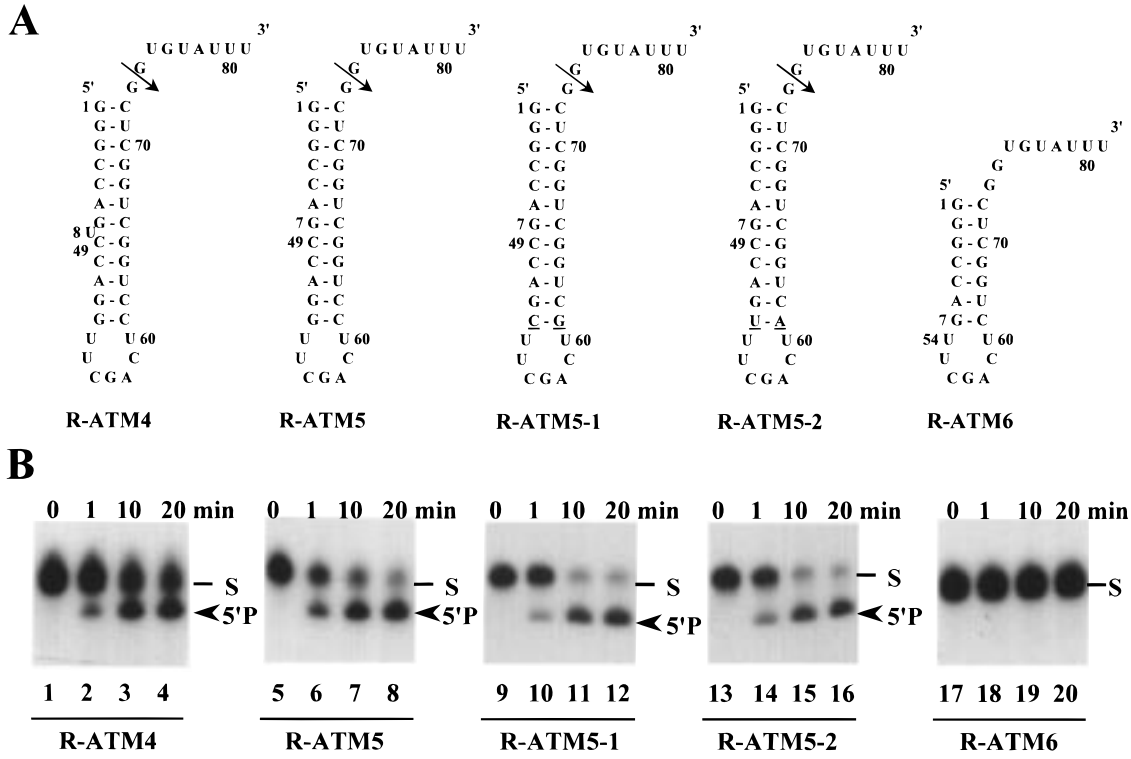

FIGURE 3: Mammalian 3′ tRNase assays for other small substrates. (A) Secondary structures of small pre-tRNA^{Arg} substrates, R-ATM4, R-ATM5, R-ATM5-1, R-ATM5-2, and R-ATM6. The acceptor stem and the T stem are connected by a single uridine residue in R-ATM4. The minihelix R-ATM5 is composed of a T stem−loop domain, an acceptor stem, a discriminator, and a 3′ trailer. The minihelices R-ATM5-1 and R-ATM5-2 differ in the underlined bases from R-ATM5. The microhelix R-ATM6 consists of a T loop, an acceptor stem, a discriminator, and a 3′ trailer. Arrows denote the cleavage sites by 3′ tRNase. (B) Pig 3′ tRNase assays. The assays were performed as described in the legend of Figure 2B.

both chains (Figure 2A). As a result, even T stem−loop domains with a decreased number of base pairs may form structures comparable to the intact T stem−loop domain. It should be noted that some of the structural changes are even favorable for the 3′ tRNase reaction (Table 1). On the other hand, in the case of the RNA complexes between T7M7 and T7HM series, those two domains were covalently connected only at one side (*13*). Consequently, as the number of T stem base pairs decreases, the RNA complexes will change structurally and lose their ability to be a 3′ tRNase substrate gradually (*13*). We further examined how T stem base pairs affect substrate recognition by 3′ tRNase using several other smaller substrates (see below).

A Minihelix Is a Good Substrate, but a Microhelix Is Not a Substrate. To elucidate the minimum requirements for mammalian 3′ tRNase substrates, we tested three smaller substrates (R-ATM4−R-ATM6) for cleavage. R-ATM4 had one uridine residue instead of the extra loop at the junction of the acceptor and T stems (Figure 3A). The minihelix R-ATM5 consisted of a T stem−loop domain, an acceptor stem, a discriminator nucleotide, and a 3′ trailer, and the microhelix R-ATM6 consisted of a T loop, an acceptor stem, a discriminator nucleotide, and a 3′ trailer (Figure 3A). The 3′ tRNase cleavage assays were performed as described above. Pig 3′ tRNase cleaved R-ATM4 as efficiently as R-UUU (Figure 3B and Table 1). The minihelix R-ATM5 was also a good substrate of 3′ tRNase, but the microhelix R-ATM6 was not a substrate (Figure 3B). The V_{max}/K_m value for the minihelix was ~1.3-fold as high as that for the wild-type R-UUU (Table 1). The catalytic efficiency of R-ATM4 and R-ATM5 was lower than that of R-ATW (Table 1), suggesting that the five-nucleotide extra loop connecting the acceptor stem and the T stem−loop domain makes the substrate more favorable for 3′ tRNase cleavage. The addition of a single uridine residue between the acceptor stem and the T stem−loop domain, however, slightly decreased the catalytic efficiency (Table 1, compare R-ATM4 and R-ATM5). The microhelix may be too short to form a stable enzyme−substrate complex.

The Conserved Bases in the T Stem Are Not Essential. Because bases G53 and C61 of the T stem are conserved in tRNAs (Figure 1), we examined the effect of base substitutions at these positions on 3′ processing. The two minihelix variants R-ATM5-1 and R-ATM5-2 that were used for this purpose contained C53·G61 and U53·A61 base pair substitutions, respectively (Figure 3A). In the 3′ tRNase assay for these minihelices, both substrates were cleaved as efficiently as their original minihelix R-ATM5 (Figure 3B), suggesting that the conserved bases at the end of the T stem are not essential for substrate recognition by 3′ tRNase.

Nucleotides in the T Loop Are Replaceable. Furthermore, we examined how the conserved and semiconserved T loop nucleotides (Figure 1) affect 3′ tRNase cleavage using five minihelix variants (R-ATM7−R-ATM11). R-ATM7−R-ATM11 contained one, two, four, six, and seven nucleotide substitutions, respectively, in the T loop: U55 to A in R-ATM7, U55 to A and A58 to U in R-ATM8, U54 to A, U55 to A, C56 to G, and U60 to C in R-ATM9, U54 to A, U55 to A, C56 to G, G57 to U, A58 to C, and U60 to G in R-ATM10, and U54 to A, U55 to A, C56 to G, G57 to U,

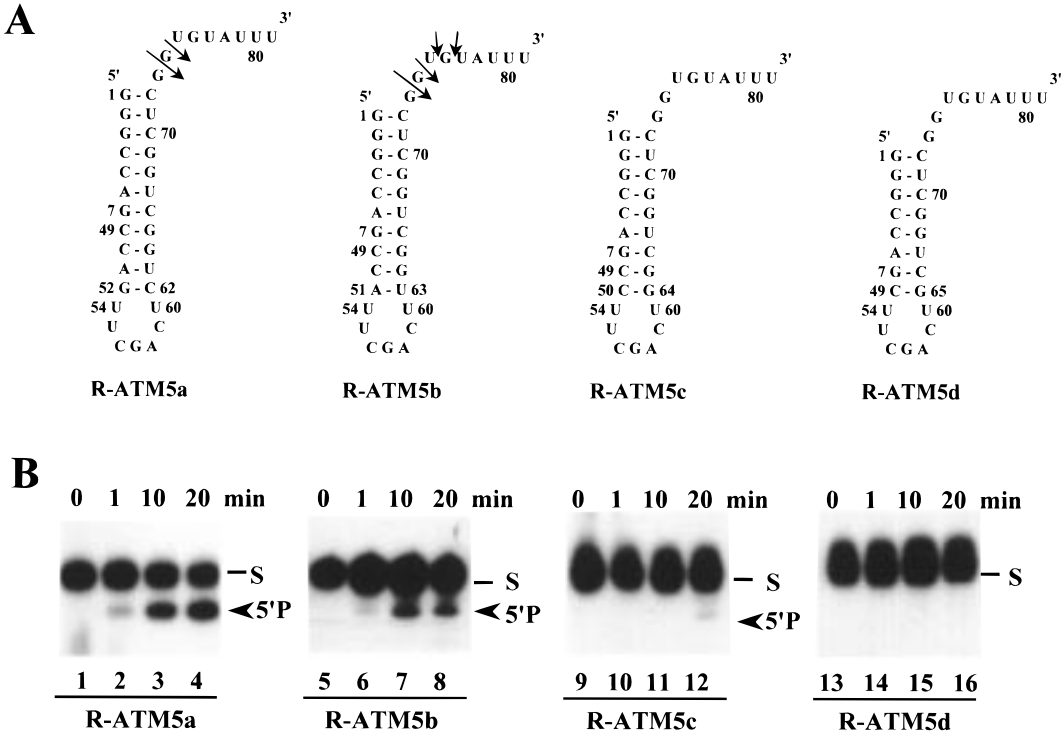

FIGURE 4: Mammalian 3′ tRNase assays for substrates R-ATM5a−R-ATM5d. (A) Secondary structures of the substrates. Arrows denote the sites of cleavage by 3′ tRNase. (B) 3′ tRNase cleavage assays. The assays were carried out as described in the legend of Figure 2B.

A58 to C, C59 to A, and U60 to G in R-ATM11. Pig 3′ tRNase cleaved all of these variants, and the relative V_{max}/K_m values of the variants were slightly smaller than that of R-ATM5 which had no nucleotide substitutions in the T loop (Table 1). The catalytic efficiency decreased with the increase in the number of nucleotide substitutions, the exception being R-ATM11 (Table 1). R-ATM11 containing substitutions of all seven nucleotides, one of which was neither conserved nor semiconserved, was cleaved more efficiently than R-ATM10 containing six nucleotide substitutions at all of the conserved or semiconserved positions (Table 1). The differences in the relative V_{max}/K_m values were small, suggesting that the nonconserved nucleotide as well as the conserved or semiconserved nucleotides in the T loop may affect the interaction between mammalian 3′ tRNase and substrate only slightly, if any. In previous experiments in which the two half-tRNA system was used, we have found that T loop nucleotide substitutions greatly affect catalytic efficiency, and that even a single U-to-A substitution at position 55 decreases the cleavage efficiency by ~3-fold (*12*). It has also been reported that base substitutions at positions 55 and 56 in the T loop severely reduce the level of in vitro *Drosophila* tRNA 3′ processing (*15*). The T loop base substitutions may affect not only direct enzyme−substrate interactions but also tertiary interactions in the full-length pre-tRNA molecule, resulting in unfavorable conformations for 3′ tRNase. On the other hand, the T loop base substitutions in the minihelix may hardly affect its conformation that is important for 3′ tRNase recognition.

The Shortest Stem Length Required for 3′ tRNase Substrates. To determine the shortest stem length required for 3′ tRNase substrates, we tested four R-ATM5 derivatives, which are shorter than the minihelix but longer than the microhelix, for cleavage. R-ATM5a containing one base pair deletion of the T stem was cleaved relatively well, although less efficiently than the original R-ATM5, while R-ATM5b containing two base pair deletions was a poor substrate (Figure 4). R-ATM5c containing three base pair deletions was hardly cleaved, and cleavage of R-ATM5d containing only an eight-base pair stem was not detected (Figure 4). These results suggest that at least an 11-base pair stem is needed for efficient substrate recognition and cleavage by mammalian 3′ tRNase.

Next, we analyzed the exact cleavage sites of R-ATM5a and R-ATM5b, because it has been shown that the pre-tRNA cleavage sites shift when the pre-tRNAs contain a total of less than 12 base pairs of the T stem and the acceptor stem (*8*). The unlabeled substrates R-ATM5, R-ATM5a, and R-ATM5b were incubated with pig 3′ tRNase at 37 °C for 10 min, and subsequently 3′-end-labeled with [5′-^{32}P]pCp and T4 ligase. The shortest 5′ cleavage product of each reaction was gel-purified (Figure 5A), and its 3′ terminal sequence was determined by the chemical RNA sequencing method (Figure 5B). Only one 5′ cleavage product was detected in the 3′ tRNase cleavage reaction of R-ATM5, while multisite cleavage was observed in the cases of R-ATM5a and R-ATM5b (Figure 5A). As expected, the cleavage of R-ATM5 occurred after the discriminator nucleotide G (Figure 5B). On the other hand, R-ATM5a was cleaved after the discriminator and less efficiently one nucleotide downstream of the discriminator, and cleavage of R-ATM5b was detected mainly after the discriminator and slightly after one, two, and three nucleotides downstream of the discriminator (Figures 4A and 5A).

The Distal Base Pairings of the T Stem Domain May Be Important. To further examine how the base pairings of the T stem domain affect substrate recognition by 3′ tRNase, we performed the in vitro 3′ tRNase cleavage assay for four

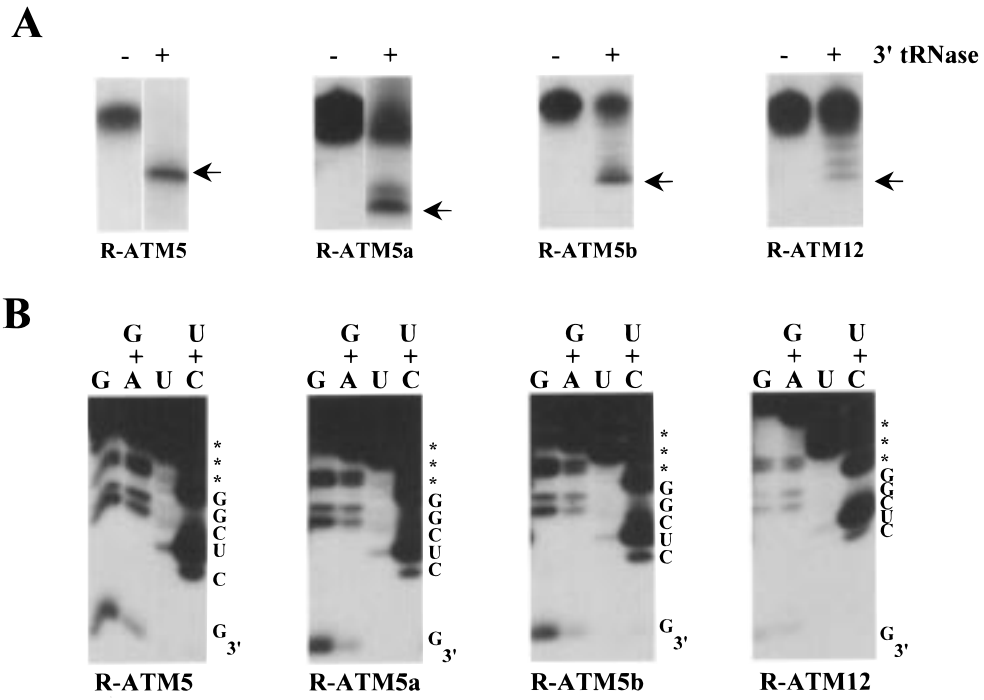

FIGURE 5: Analysis of cleavage sites for substrates R-ATM5, R-ATM5a, R-ATM5b, and R-ATM12. (A) The 3′-end labeling of the 3′ tRNase cleavage products. After the reaction of each cold pre-tRNA substrate with (+) or without (−) pig 3′ tRNase, the products were 3′-end-labeled with [5′-^{32}P]pCp and T4 ligase, and separated on a denaturing gel. Arrows denote the smallest 5′ products of cleavage by 3′ tRNase. (B) Chemical RNA sequencing for the smallest cleavage products. The 3′ terminal sequence of each smallest 5′ cleavage product is shown in the right-hand column.

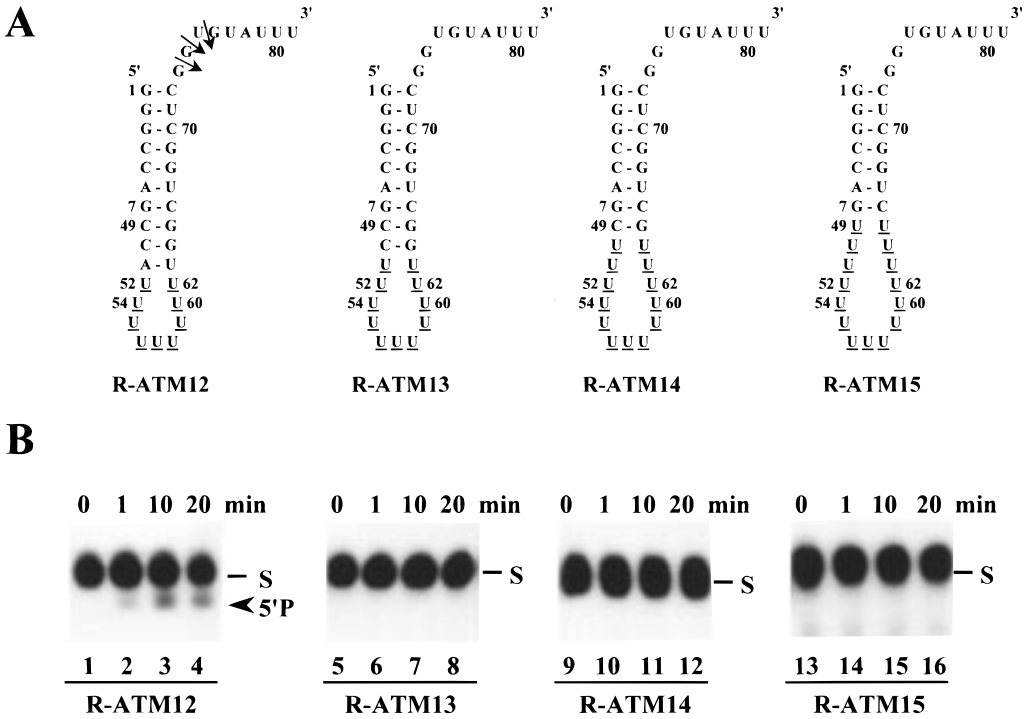

FIGURE 6: Mammalian 3′ tRNase assays for pre-tRNA substrates derived from R-ATM5a. (A) Secondary structures of substrates R-ATM12−R-ATM15. Arrows and underlines denote the sites of cleavage by 3′ tRNase and substituted nucleotides, respectively. (B) 3′ tRNase cleavage reactions. The reactions were performed as described in the legend of Figure 2B.

substrates derived from R-ATM5a, which was shown to be a minimum substrate (Figure 4). The four derivatives R-ATM12−R-ATM15 contained one, two, three, and four base pairing disruptions, respectively, in the T stem domain because the paired bases were replaced with uridines (Figure 6A). In addition, all of the T loop bases of these substrates were changed to uridines to avoid unexpected base pairings in the loop region (Figure 6A). In the standard time course analysis, R-ATM12 was slightly cleaved by 3′ tRNase, while cleavage of the other three substrates was not detected (Figure 6B). These results suggest that distal base pairings in the T stem domain may be important for enzyme recognition, although changing the sequence to all uridines in the T loop may have had an effect. This observation

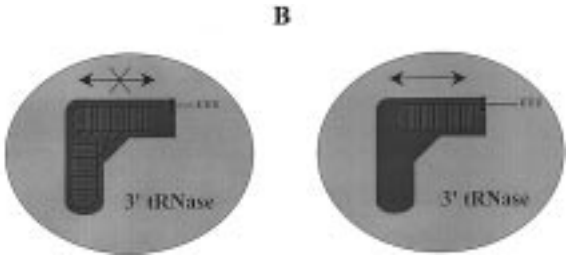

FIGURE 7: Schematic drawings of a model for the interaction between mammalian 3′ tRNase and the pre-tRNA substrate. A region of 3′ tRNase that binds to the L-shaped mature tRNA domain and the catalytic domain are represented by a dark shaded area and triangles, respectively. (A) It is likely that pre-tRNAs containing a bottom-half domain are prevented from moving in the directions indicated by an arrow due to the bottom-half domain constraints. (B) On the other hand, pre-tRNAs without a bottom-half domain are likely able to move in the indicated directions relatively easily.

contrasts sharply with the fact that proximal base pairings in the T stem domain are dispensable for recognition by mammalian 3′ tRNase (Figure 2).

The exact cleavage site of R-ATM12 was determined as described above. Three 5′ cleavage products were detected as bands with nearly the same intensity (Figure 5A). RNA sequencing for the smallest 5′ cleavage product revealed that the cleavage of R-ATM12 occurred not only after the discriminator nucleotide G but also after one and two nucleotides downstream of the discriminator (Figures 5 and 6A).

Minimum Substrates for Mammalian 3′ tRNase. In the experiments in which various small pre-tRNA^{Arg} derivatives were used, we demonstrated that mammalian 3′ tRNase can efficiently cleave 14 of 22 substrates, most of which were shown to be better substrates than the full-length wild-type R-UUU (Table 1). Cleavage of the two substrates R-ATM5b and R-ATM12 was much less efficient, and the other six small substrates were hardly cleaved or not at all. Taken together, our results suggest that minimum substrates for mammalian 3′ tRNase are minihelices or "minihelicesΔ1" (such as R-ATM5a) that are one base pair smaller than minihelices and are less efficient substrates. In these minimum substrates, there are no essential bases in the T loop domain and the most distal T stem base pair. It is also highly likely that there are no base constraints in the acceptor stem domain and the other T stem domain, since tRNAs do not have any conserved or semiconserved bases in these domains (*16*). Furthermore, as we showed above (Figure 2), some of the proximal base pairings in the T stem are unnecessary, and some of the proximal acceptor stem base pairings may be also dispensable. The length of the T loop may be able to be shortened, although we did not address this issue in this study.

Cleavage Site Selection in Small Pre-tRNAs. We have found a general rule for cleavage site selection by mammalian 3′ tRNase with respect to pre-tRNAs containing D stem−loop and anticodon stem−loop domains as well as T stem−loop and acceptor stem domains (*8*). According to this rule, cleavage of pre-tRNAs containing a total of *N* base pairs ($N < 12$) in the acceptor stem and the T stem occurs after $12 - N$ and $13 - N$ nucleotides 3′ to the discriminator, while cleavage of pre-tRNAs with a total of *N* base pairs ($N \geq 12$) occurs after the discriminator (*8*).

In this study, we found that cleavage of small pre-tRNAs with a total of less than 12 base pairs in the acceptor stem and the T stem (R-ATM5a, R-ATM5b, and R-ATM12) occurs at multiple sites (Figures 4−6). The cleavage sites, however, did not strictly obey the selection rule: R-ATM5a, at nucleotides 73 and 74 (nucleotides 74 and 75 expected); R-ATM5b, at nucleotides 73−76 (nucleotides 75 and 76 expected); and R-ATM12, at nucleotides 73−75 (nucleotides 75 and 76 expected). In the cases of these small pre-tRNAs, the cleavage sites generally fluctuated between the discriminator nucleotide and $12 - N$ or $13 - N$ nucleotides (*N* is the total number of base pairs in the acceptor stem and the T stem) 3′ to the discriminator.

These results suggest that pre-tRNAs containing a total of less than 12 base pairs in the acceptor stem and the T stem can slide along the "top-half tRNA" (acceptor stem and the T stem−loop domain) binding domain on 3′ tRNase in the absence of the "bottom-half tRNA" (D stem−loop domain and anticodon stem−loop domain) (Figure 7B). On the other hand, pre-tRNAs with 12 base pairs cannot slide probably due to the limited space for binding of the top-half tRNA domain (Figure 7) (*8*). Cleavage at the discriminator was predominant in R-ATM5a and R-ATM5b, while cleavage of R-ATM12 occurred evenly at any cleavable sites (Figure 5A). This observation implies that contrary to our previous model (*8*), the former two small pre-tRNAs tend to bind to the enzyme in such a way that the distal acceptor stem is located in the vicinity of the catalytic domain rather than in a way that the T loop is arranged at its original binding site (Figure 7). This tendency, however, seems to change depending on the T loop structures as seen in R-ATM12.

In the case of pre-tRNAs containing a bottom-half domain as well as a total of less than 12 base pairs in the acceptor stem and the T stem, we have demonstrated that the T loop region tends to make the original interactions with 3′ tRNase, resulting in destruction of the original interaction between the distal acceptor stem and the enzyme (*8*). Taken together, our results suggest that this type of interaction which is different from that in the small pre-tRNAs can be attributed primarily to the presence of the bottom-half tRNA domain (Figure 7).

Cleavage of R-ATM1 and R-ATM2, which contain proximal one and two base pair disruptions, respectively, in the T stem domain (Figure 2A), occurred after the discriminator G (data not shown). This observation suggests that small pre-tRNAs containing proximal base pair disruptions behave like a substrate with 12 intact base pairs, and that mammalian 3′ tRNase can select the cleavage site in a fashion similar to that of their original small substrate.

Evolutionary Considerations. Minihelices have been shown to be sufficient for the interactions with many proteins that are important for tRNA metabolism. These proteins include RNase P (*17*), aminoacyl tRNA synthetases (*18*), elongation factor Tu (*19*), and tRNA nucleotidyltransferase (*20*). On the basis of these observations and others, a hypothesis has been proposed that the tRNA minihelix domain evolved independent of the other domain composed of the D and anticodon stem−loop domains (*21*−*23*). Our conclusion that minihelices are sufficient for recognition by mammalian 3′ tRNase may provide additional support for this hypothesis.

ACKNOWLEDGMENT

We thank S. Geary for technical assistance.

REFERENCES

1. Sprague, K. U. (1995) in *tRNA: Structure, Biosynthesis, and Function* (Söll, D., and RajBhandary, U. L., Eds.) pp 31−50, American Society for Microbiology, Washington, DC.
2. Altman, S., Kirsebom, L., and Talbot, S. (1995) in *tRNA: Structure, Biosynthesis, and Function* (Söll, D., and RajBhandary, U. L., Eds.) pp 67−78, American Society for Microbiology, Washington, DC.
3. Nashimoto, M. (1997) *Nucleic Acids Res. 25*, 1148−1155.
4. Deutscher, M. P. (1995) in *tRNA: Structure, Biosynthesis, and Function* (Söll, D., and RajBhandary, U. L., Eds.) pp 51−65, American Society for Microbiology, Washington, DC.
5. Deutscher, M. P. (1990) *Prog. Nucleic Acids Res. Mol. Biol. 39*, 209−240.
6. Mohan, A., Whyte, S., Wang, X., Nashimoto, M., and Levinger, L. (1999) *RNA 5*, 245−256.
7. Nashimoto, M., Wesemann, D. R., Geary, S., Tamura, M., and Kaspar, R. L. (1999) *Nucleic Acids Res. 27*, 2770−2776.
8. Nashimoto, M., Tamura, M., and Kaspar, R. L. (1999) *J. Mol. Biol. 287*, 727−740.
9. Nashimoto, M. (1992) *Nucleic Acids Res. 20*, 3737−3742.
10. Nashimoto, M. (1993) *Nucleic Acids Res. 21*, 4696−4702.
11. Nashimoto, M. (1995) *Nucleic Acids Res. 23*, 3642−3647.
12. Nashimoto, M. (1996) *RNA 2*, 523−534.
13. Nashimoto, M., Geary, S., Tamura, M., and Kaspar, R. (1998) *Nucleic Acids Res. 26*, 2565−2571.
14. Peattie, D. A. (1979) *Proc. Natl. Acad. Sci. U.S.A. 76*, 1760−1764.
15. Levinger, L., Bourne, R., Kolla, S., Cylin, E., Russell, K., Wang, X., and Mohan, A. (1998) *J. Biol. Chem. 273*, 1015−1025.
16. Dirheimer, G., Keith, G., Dumas, P., and Westhof, E. (1995) in *tRNA: Structure, Biosynthesis, and Function* (Söll, D., and RajBhandary, U. L., Eds.) pp 93−126, American Society for Microbiology, Washington, DC.
17. McClain, W. H., Guerrier-Takada, C., and Altman, S. (1987) *Science 238*, 527−530.
18. Schimmel, P., and Ribas de Pouplana, L. (1995) *Cell 81*, 983−986.
19. Rudinger, J., Blechschmidt, B., Ribeiro, S., and Sprinzl, M. (1994) *Biochemistry 33*, 5682−5688.
20. Shi, P.-Y., Weiner, A. M., and Maizels, N. (1998) *RNA 4*, 276−284.
21. Schimmel, P., Giege, R., Moras, D., and Yokoyama, S. (1993) *Proc. Natl. Acad. Sci. U.S.A. 90*, 8763−8768.
22. Noller, H. F. (1993) in *The RNA world* (Gesteland, R. F., and Atkins, J. F., Eds.) pp 137−156, Cold Spring Harbor Laboratory Press, Plainview, NY.
23. Maizels, N., and Weiner, A. M. (1993) in *The RNA world* (Gesteland, R. F., and Atkins, J. F., Eds.) pp 577−602, Cold Spring Harbor Laboratory Press, Plainview, NY.

BI9911942